

# Adsorption of metal-phthalocyanine molecules onto the Si(111) surface passivated by $\delta$ doping: *Ab initio* calculations

R. G. A. Veiga

*Departamento de Engenharia Metalúrgica e de Materiais, Escola Politécnica, Universidade de São Paulo, Avenida Prof. Mello de Moraes, 2463, CEP 05508-030, São Paulo, São Paulo, Brazil*

R. H. Miwa\*

*Instituto de Física, Universidade Federal de Uberlândia, Caixa Postale 593, 38400-902, Uberlândia, Minas Gerais, Brazil*

A. B. McLean

*Department of Physics, Engineering Physics and Astronomy, Queen's University, Kingston, Ontario, Canada K7L 3N6*  
(Received 27 October 2015; revised manuscript received 29 January 2016; published 1 March 2016)

We report first-principles calculations of the energetic stability and electronic properties of metal-phthalocyanine (MPc) molecules ( $M = \text{Cr, Mn, Fe, Co, Ni, Cu, and Zn}$ ) adsorbed on the  $\delta$ -doped Si(111)-B( $\sqrt{3} \times \sqrt{3}$ ) reconstructed surface. (i) It can be seen that CrPc, MnPc, FePc, and CoPc are chemically anchored to the topmost Si atom. (ii) Contrastingly, the binding of the NiPc, CuPc, and ZnPc molecules to the Si(111)-B( $\sqrt{3} \times \sqrt{3}$ ) surface is exclusively ruled by van der Waals interactions, the main implication being that these molecules may diffuse and rearrange to form clusters and/or self-organized structures on this surface. The electronic structure calculations reveal that in point (i), owing to the formation of the metal-Si covalent bond, the net magnetic moment of the molecule is quenched by  $1\mu_B$ , remaining unchanged in point (ii). In particular, the magnetic moment of CuPc ( $1\mu_B$ ) is preserved after adsorption. Finally, we verify that the formation of ZnPc, CuPc, and NiPc molecular (self-assembled) arrangements on the Si(111)-B( $\sqrt{3} \times \sqrt{3}$ ) surface is energetically favorable, in good agreement with recent experimental findings.

DOI: [10.1103/PhysRevB.93.115301](https://doi.org/10.1103/PhysRevB.93.115301)

## I. INTRODUCTION

In the past quarter of a century, self-assembled monolayers of organic molecules have emerged as an important nanotechnology. The growth of self-assembled monolayers (SAMs) depends sensitively on the weak noncovalent interactions between molecules, steric effects, and the interaction of the molecules in the layer with the surface. The low-index crystalline surfaces of noble metals have served as a convenient platform for studying the surface-confined self-assembly of small organic molecules [1–5]. Although noble-metal surfaces do not, as a general rule, provide unsurmountable kinetic barriers to aggregation and self-assembly, this is not true of silicon surfaces [6,7], where surface reactivity and diffusion barriers impede the growth of supramolecular arrays. Therefore, one cannot employ supramolecular assembly methodologies, which are contingent on the use of passive surfaces, to design hybrid silicon-organic devices that would take advantage of the versatile biofunctional and optical properties of organic materials [8,9].

Consequently, the recent discovery [10–13] that small organic molecules can be assembled into supramolecular arrays on Si(111) surfaces that are passivated by B  $\delta$  doping [14–18] is of considerable importance to the study of self-assembly on Si. Although it has been known for many years [19–21] that the Si surface can be passivated by adsorbing noble-metal atoms, like Ag, onto Si(111),  $\delta$  doping affords the opportunity of studying self-assembly directly on an atomic layer of Si

atoms without the complication of an interlayer because the  $\delta$ -doped B layer lies just below the surface.

Among the many small organic molecules that are potential candidates for forming SAMs on the  $\delta$ -doped Si(111) surface, polyaromatic phthalocyanine (Pc) is one of particular interest. In its ionic form ( $\text{C}_{32}\text{H}_{16}\text{N}_8^{2-}$ ), Pc is able to accommodate in its central cavity atoms or groups of atoms in their 2+ oxidation state. Transition-metal atoms, for instance, are routinely incorporated in that position, and this has important implications for the electronic, magnetic, and/or chemical behavior of the resulting molecule [22]. A number of recent theoretical and experimental studies address the adsorption of transition-metal phthalocyanine molecules on metallic and semiconducting surfaces [23–28].

The focus of this study is a theoretical investigation of the adsorption of a wide range of metal-phthalocyanine (MPc) molecules on the B-passivated Si(111) reconstructed surface. We examine the bonding between the surface and the adsorbate and the tenacity of the magnetic moment located on the metal atom to adsorption. We also explore, by studying the coupling between the molecules, the formation of SAMs of MPc molecules on this surface, recently observed for ZnPc and CuPc with scanning probe microscopy [24].

## II. METHOD

The calculations were performed using the density functional theory (DFT) as implemented in the QUANTUM ESPRESSO package [29]. Exchange correlation was calculated using the generalized gradient approximation (GGA) including the van der Waals (vdW) correction based on the nonlocal density

\*hiroki@infis.ufu.br

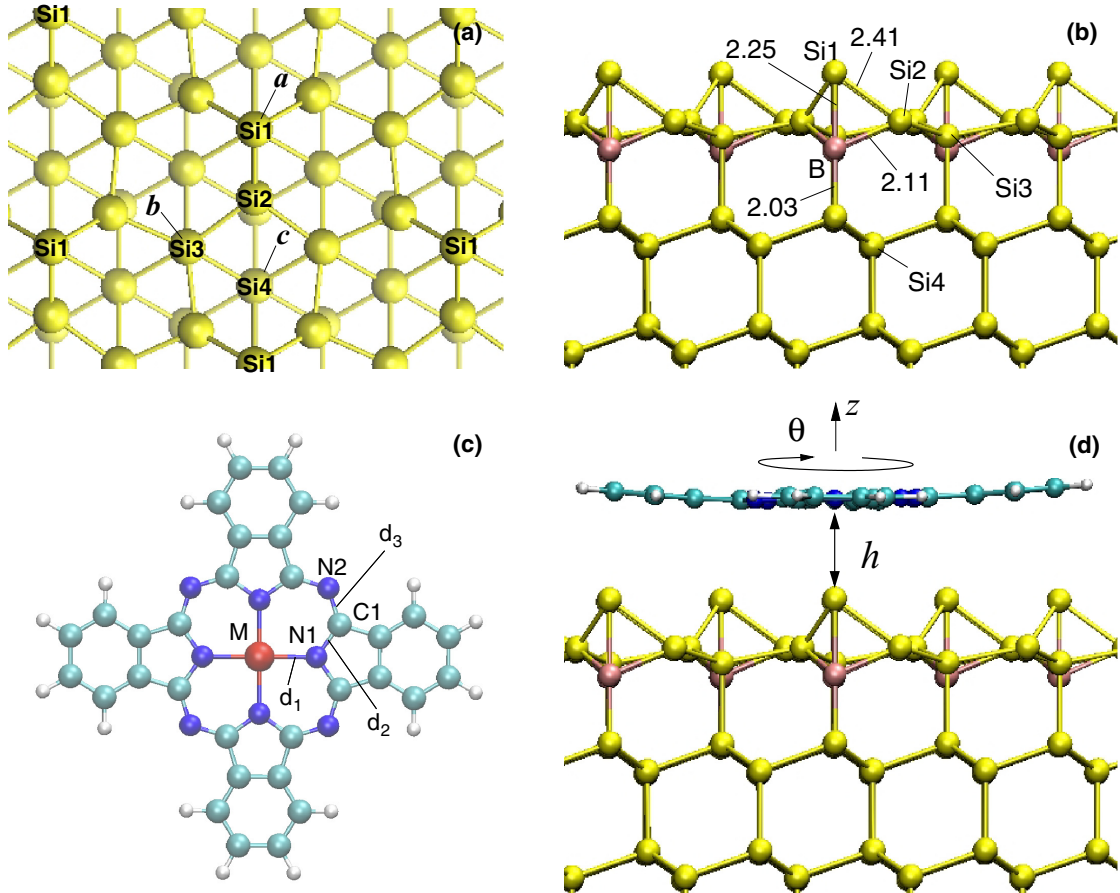


FIG. 1. Structural model of the Si(111)-B( $\sqrt{3} \times \sqrt{3}$ ) surface in both (a) top and (b) side views. The *MPc* adsorption sites are labeled *a*, *b*, and *c*. In each *MPc*/SiB configuration, the central metal atom in the molecule is situated directly above one of the adsorption sites. The atomic distances are in angstroms. (c) Equilibrium geometry of an isolated *MPc* molecule. (d) A side view of a *MPc* molecule adsorbed on site *a*.

functionals proposed in Refs. [30–32]. The Kohn-Sham orbitals were expanded in plane-wave basis sets with an energy cutoff of 380 eV, checked up to 435 eV with energy differences within 10 meV/cell. To relax the geometry of the systems, the self-consistent total charge density was calculated using the  $\Gamma$  point. The charge transfer and projected density of states (PDOS), in turn, were calculated with a  $3 \times 3 \times 1$  *k*-point mesh generated according to the Monkhorst-Pack scheme [33].

The Si(111)-B( $\sqrt{3} \times \sqrt{3}$ ) surface (hereafter, SiB) was represented by slabs comprising seven Si monolayers with B atoms just below the topmost layer and the bottom layer being passivated by hydrogen atoms. The periodicity of the surface unit cell was  $\sqrt{3} \times \sqrt{3}$ , with a lattice parameter of 6.7 Å. Depending on the geometry of the adsorbed system, the surface supercell was hexagonal or square. A vacuum region of 23 Å was introduced in the direction perpendicular to the SiB surface to prevent spurious interactions between the system and its images.

### III. RESULTS

#### A. SiB surface and isolated *MPc* molecules

Initially, we examined some key structural and electronic properties of the isolated systems: the SiB surface and the *MPc* molecule. Our calculated equilibrium geometry for

TABLE I. M-N1 equilibrium bond length  $d_1$  (Å) in Fig. 1(c) and the net magnetic moment (*m* in units of  $\mu_B$ ) for isolated *MPc*.

| Molecule | $d_1$ | <i>m</i> |
|----------|-------|----------|
| CrPc     | 1.95  | 4.0      |
| MnPc     | 1.94  | 3.0      |
| FePc     | 1.93  | 2.0      |
| CoPc     | 1.92  | 1.0      |
| NiPc     | 1.92  | 0.0      |
| CuPc     | 1.98  | 1.0      |
| ZnPc     | 2.01  | 0.0      |

the SiB surface [Figs. 1(a) and 1(b)] agrees with previous experimental and theoretical results [34,35]. The surface has a semiconducting character, where the silicon atoms Si1 and Si2 contribute to the formation of the highest occupied and the lowest unoccupied states [36]. In Table I, we summarize our results for isolated *MPc* molecules. At the equilibrium geometry, we find M-N1 bond lengths [ $d_1$  in Fig. 1(c)] in the range 1.92–2.01 Å, and our calculated magnetic moments *m* are in good agreement with previous theoretical estimates [37–41] and experimental results [42–46]. Five *MPc* molecules presented a net magnetization varying from  $1\mu_B$  to  $4\mu_B$  (NiPc and ZnPc, in turn, showed  $m = 0$ ), but we verified that there

are differences in the origin of their magnetic moments. To illustrate that, in Figs. 2(a) and 2(c) we present the PDOS on the metal atoms of isolated CoPc and CuPc molecules. Both molecules have magnetic moments of around  $1\mu_B$ . However, those two molecules have a different electronic distribution; namely, in CoPc, most of the spin polarization is due to the partial occupation of Co  $3d_{z^2}$  orbitals, with a negligible contribution from the N  $2p$  orbitals nearest the central metal atom. Contrastingly, the N  $2p$  orbitals of the inner ring of CuPc become spin polarized ( $m = 0.13\mu_B/\text{N atom}$ ), and the net magnetization of the central Cu atom ( $0.44\mu_B$ ) is mostly attributed to the  $3d_{x^2-y^2}$  and  $3d_{xy}$  orbitals. Those differences will influence the molecule-surface interaction and the electronic properties of the adsorbed molecule.

### B. Single MPC molecules adsorbed on SiB

Next, we investigated the adsorption of a single MPC molecule onto the SiB surface. The substrate was represented by a hexagonal slab comprising 16 (i.e.,  $4 \times 4$ ) unit cells. The minimum separation between the H atoms at the ends of the molecule and the closest H atoms in adjacent periodic images was about 12 Å. This corresponds to a lateral distance of about 27 Å between the central metal atoms of neighboring MPC molecules. Therefore, molecule-molecule interactions can be considered negligible in the energetic analysis. The energetic stability of the MPC/SiB system was examined by comparing the total energy of the combined system MPC/SiB  $E[\text{MPC/SiB}]$  with the total energies of the completely separated components: the MPC molecule ( $E[\text{MPC}]$ ) and the SiB surface ( $E[\text{SiB}]$ ),

$$E^a = E[\text{MPC}] + E[\text{SiB}] - E[\text{MPC/SiB}].$$

Positive values of the adsorption energy  $E^a$  indicate an exothermic process. Here we have considered three plausible adsorption sites, *a*, *b*, and *c* in Fig. 1(a). Site *a* deserves special attention because it is directly above one of the topmost Si adatoms (Si1). Therefore, it is expected to be the most chemically reactive site in spite of the fact that B  $\delta$  doping passivates the surface. In the adsorbed configurations, the molecule lays down parallel to the surface, with the metal atom on top of one of the adsorption sites. The equilibrium molecule-surface separation  $h$  was taken as the vertical distance between the metal atom in the molecule and the topmost Si atom layer on the SiB surface [Fig. 1(d)]. Our results for  $E^a$  and  $h$  are summarized in Table II. We find that CrPc, MnPc, FePc, and CoPc molecules prefer to have the metal atom on top of the Si1 adatom in site *a*. For those molecules, the calculated vertical distances are close to the sum of the covalent radii of Si and the metal atom of the MPC molecule (2.33–2.35 Å), indicating that MPC-SiB chemical bonds are formed. Here the formation of M-Si1 chemical bonds in the CrPc/, MnPc/, FePc/, and CoPc/SiB systems can be attributed to the partial occupation of the M  $3d_{z^2}$  orbital. The other sites, *b* and *c*, are found to be 0.8–1 eV less stable and are characterized by a larger separation ( $>3$  Å) between the molecule and the substrate. This suggests they are physisorbed metastable configurations.

The strength of the MPC-SiB chemical interaction can also be pictured through the differential charge density  $\Delta\rho$  at the

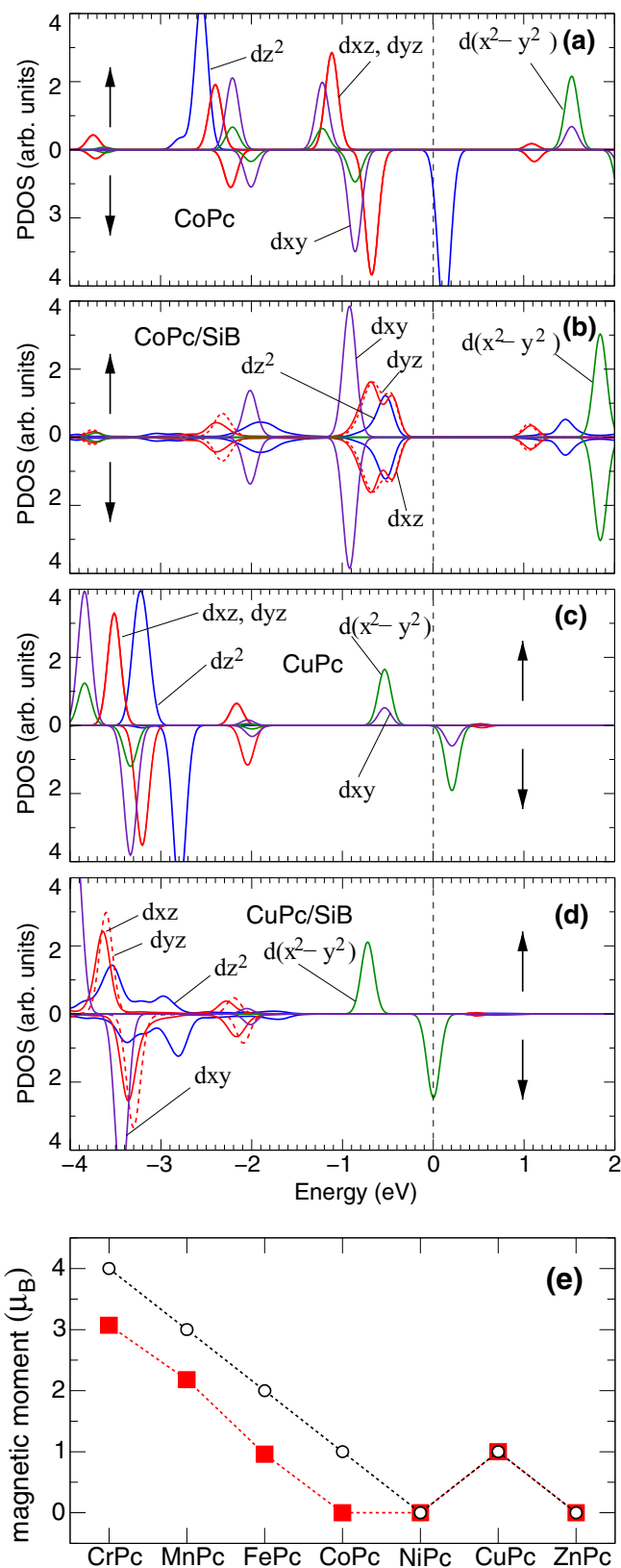


FIG. 2. The calculated projected density of states (PDOS) on (a) Co and (c) Cu atoms of an isolated MPC molecule. (b) PDOS on the Co atom of a CoPc adsorbed on SiB. (d) PDOS on the Cu atom of a CuPc adsorbed on SiB. (e) The calculated net magnetic moment of isolated (open circles) and adsorbed surface (solid squares) MPC molecules.

TABLE II. Adsorption energies (in eV/MPC molecule) for MPC on SiB adsorption sites  $a$  ( $E^a[a]$ ),  $b$  ( $E^a[b]$ ), and  $c$  ( $E^a[c]$ ), shown in Fig. 1(a), and the M-Si1 equilibrium vertical distance (in Å), indicated as  $h$  in Fig. 1(d), for the most stable configuration.

| Molecule | $E^a[a]$ | $E^a[b]$ | $E^a[c]$ | $h$  |
|----------|----------|----------|----------|------|
| CrPc     | 2.93     | 1.93     | 1.90     | 2.39 |
| MnPc     | 2.91     | 1.92     | 1.87     | 2.34 |
| FePc     | 2.97     | 2.02     | 1.97     | 2.30 |
| CoPc     | 2.89     | 2.08     | 2.03     | 2.33 |
| NiPc     | 1.95     | 1.85     | 1.77     | 2.80 |
| CuPc     | 1.89     | 1.90     | 1.82     | 2.97 |
| ZnPc     | 1.79     | 1.84     | 1.76     | 3.03 |

MPC-SiB interface, where  $\Delta\rho$  can be written as

$$\Delta\rho = \rho_{\text{MPC/SiB}} - \rho_{\text{MPC}} - \rho_{\text{SiB}}.$$

$\rho_{\text{MPC/SiB}}$  represents the total charge density of the MPC/SiB system, and  $\rho_{\text{MPC}}$  and  $\rho_{\text{SiB}}$  are the total charge densities of the isolated components. In Fig. 3(a) we present our  $\Delta\rho$  result for the CoPc/SiB system. We find that the electronic charge redistribution takes place not only at the CoPc-SiB interface (being mostly aligned with the central pyrrolic ring bonded to the transition metal) but also below the SiB surface. There is a net charge-density gain on the Co atom, and the magnetic moment of the Co  $3d_{z^2}$  orbital is completely quenched ( $m = 1\mu_B \rightarrow 0\mu_B$ ), as shown in Figs. 2(b) and 2(e). Indeed, such a reduction (of  $1\mu_B$ ) on the MPC magnetic moment, mediated by the MPC-SiB interaction, was also verified for CrPc/, MnPc/, and FePc/SiB [Fig. 2(e)].

In contrast, the net magnetic moment of NiPc, CuPc, and ZnPc is unchanged by adsorption [Fig. 2(e)]. Moreover, the adsorption energies for NiPc, CuPc, and ZnPc on site  $a$  are lower than the adsorption energies of their counterpart molecules on the same site by about 1 eV and are similar to the adsorption energies on sites  $b$  and  $c$  (see Table II). At the equilibrium geometry, the vertical distances  $h$  are larger

(by  $\sim 0.6$  Å) than the sum of the covalent radii of Si and the metal atom of MPC. The weak interaction between the CuPc molecule and the SiB surface, when compared with, for instance, CoPc/SiB, can be verified by mapping the differential charge density at the CuPc-SiB interface [Fig. 3(b)]. Here we find a charge-density redistribution localized at the molecule-surface interface region, around the Cu atom of CuPc.

Although the interaction between the CuPc molecule and the SiB surface is weak, the  $D_{4h}$  symmetry of the molecule has been removed, promoting a small energy splitting of the  $E_g$  levels, composed of  $3d_{xz}$  and  $3d_{yz}$  orbitals. In Fig. 2(d), we present the PDOS of CuPc/SiB, where (i) the degeneracy of the Cu  $3d_{xz}$  and  $3d_{yz}$  orbitals has been removed and (ii) the occupied Cu  $3d_{z^2}$  orbital has been perturbed due to its interaction with the SiB surface.

The interaction with the SiB surface provoked distortions on the molecules. The deviations from the planar structure of the isolated MPCs, however, were relatively small. Notably, for the chemisorbed configurations, the central metal atom moved towards the topmost Si atom to form the chemical bond, whereas the benzene rings at the molecule ends displaced upwards, resulting in a slightly convex geometry. Strain energies [47] were in the 70–100 meV range for the chemisorbed molecules and below 50 meV for the physisorbed configurations.

### C. Self-assembly

The self-assembly of MPC molecules onto metallic and semiconducting surfaces has been the subject of a number of experiments. CuPc, for instance, has been observed to form self-assembled square arrays parallel to the Ag(100) surface [27]. Of special interest, however, is the work of Wagner *et al.* [24]. Using scanning probe microscopy, the authors investigated the self-assembling of ZnPc and CuPc molecules on SiB. Favored by low molecular diffusion barriers even at room temperature and the presence of step edges, linear stripes of tilted MPC molecules on the surface terraces were observed.

CuPc/SiB seems particularly interesting for the investigation of self-assembly since its net magnetic moment is preserved upon adsorption and, as shown in Table II, the adsorption energy differences on sites  $a, b$ , and  $c$  are less than 0.09 eV and therefore very small compared to the differences seen for CoPc, for instance. Additionally, for each adsorption site, we calculated the adsorption energy as a function of the CuPc rotation around an axis perpendicular to the molecular plane and passing through the Cu atom. For rotation steps of  $15^\circ$  [ $\theta = 0 \rightarrow 90^\circ$  in Fig. 1(d)], we find  $E^a$  differences of 0.05 eV for the CuPc molecule lying on site  $a$  ( $\Delta E[a] = 0.05$  eV), and  $\Delta E[b] = 0.06$  eV and  $\Delta E[c] = 0.10$  eV. Altogether, these results suggest that CuPc molecules are free to displace and rotate on the SiB surface, necessary requirements for self-assembling [48] that are not entirely fulfilled, according to our calculations, by the other magnetic molecules (CrPc, CoPc, FePc, and MnPc). One should expect (and this is indeed experimentally observed for ZnPc, as mentioned in the previous paragraph) that these requirements are also obeyed by NiPc and ZnPc. However, these molecules lack net magnetization.

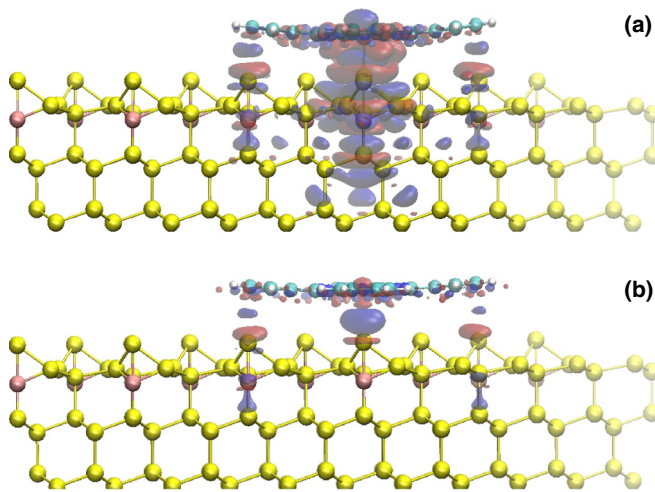


FIG. 3. Total charge difference  $\Delta\rho$  of (a) CoPc/SiB and (b) CuPc/SiB. Blue and red indicate  $\Delta\rho > 0$  and  $\Delta\rho < 0$ , respectively. The isosurfaces correspond to a charge density of  $\pm 5 \times 10^{-4} e/a_0^3$ .

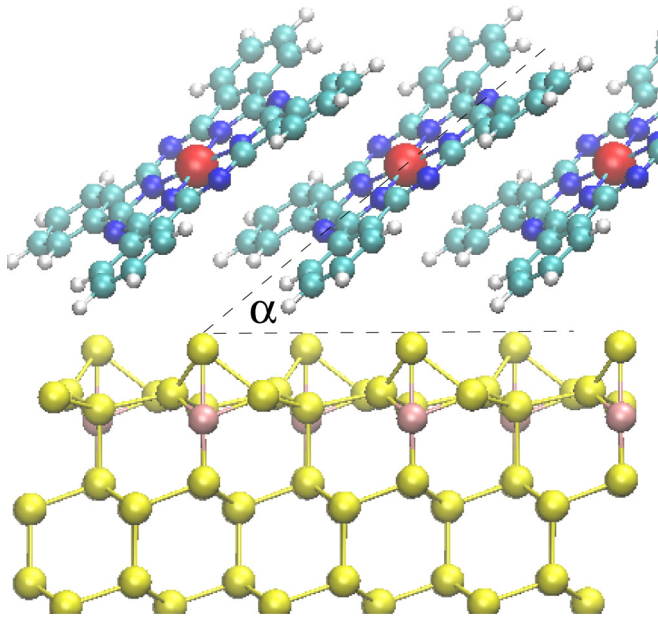


FIG. 4. Structural models of self-assembled ML composed by linear stripes of CuPc on the SiB surface, as proposed in Ref. [24].

Following the structural model proposed in Ref. [24], with tilted rather than planar orientation of the adsorbed molecules, we calculate the equilibrium geometry, the adsorption energy, and electronic properties of NiPc, ZnPc, and CuPc molecules forming a monolayer (ML) of molecular stripes on the SiB surface (MPc stripe/SiB, with  $M = \text{Ni, Zn, and Cu}$ ) [49]. Initially, taking into account the fact that there is no obvious adsorption site when the molecule is tilted with respect to the surface, we have considered six different CuPc stripe/SiB configurations for which the position of the molecule above the surface was chosen at random. After relaxation, we find an  $E^a$  of 2.33 eV/molecule for the most stable configuration, as shown in Fig. 4, with the second (2.31 eV/molecule) and third (2.30 eV/molecule) most stable geometries very close in energy. The  $E^a$  of the least stable geometry, in turn, was 2.08 eV/molecule. At the equilibrium geometry, the CuPc molecule is inclined by around  $38^\circ$  with respect to the (111) surface plane (indicated as  $\alpha$  in Fig. 4). The intermolecular distance was 4.1 Å, whereas the shortest separation between an atom in the molecule and the surface was about 2.3 Å. The other MPc/SiB systems present similar equilibrium geometry, and we find adsorption energies of 2.30 and 2.27 eV/molecule for NiPc stripe/ and ZnPc stripe/SiB, respectively. Experimental measurements indicate an inclination of ZnPc molecules of  $\sim 30^\circ$  [24]. Here, comparing with the adsorption energies presented in Table II, we verify that the MPc stripe/SiB structures are energetically more stable than their counterpart single MPC molecules adsorbed parallel to the surface [as shown in Fig. 1(d)]. There is no chemical bonding between the molecules or between the molecule and the surface in MPc stripe/SiB, indicating that the self-assembly of MPc linear structures on SiB is ruled solely by the vdW interaction.

In Fig. 5, we present the total DOS and PDOS on the M  $3d$  and N  $2p$  orbitals. The DOSs of NiPc stripe/ and ZnPc stripe/SiB systems indicate that the semiconducting character

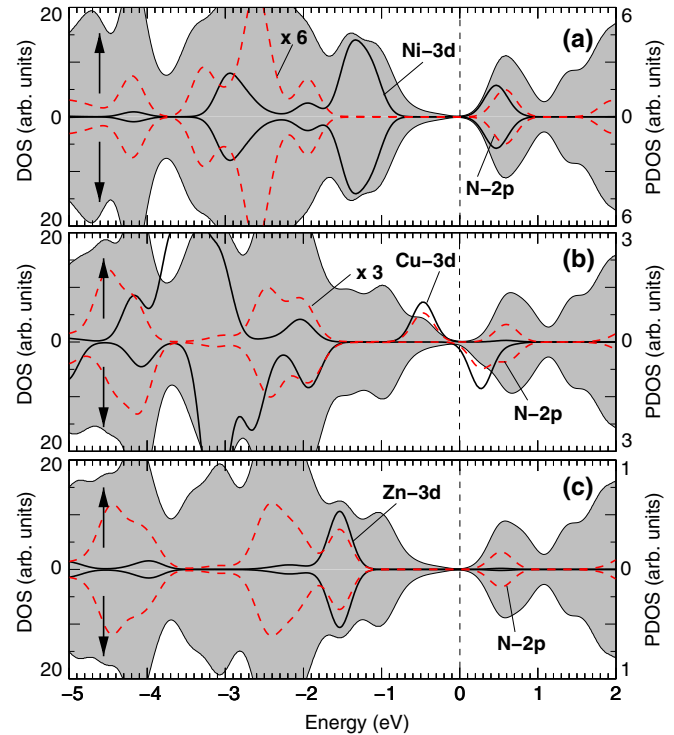


FIG. 5. Total DOS (shaded area) and the projected DOS (PDOS) on the metal  $3d$  and N  $2p$  orbitals of (a) NiPc/SiB, (b) CuPc/SiB, and (c) ZnPc/SiB.

of the SiB surface has been preserved upon the formation of a ML of MPc stripes [Figs. 5(a) and 5(c)]. Meanwhile, we find Cu  $3d$  and N  $2p$  unpaired orbitals within the band gap of the SiB surface [Fig. 5(b)]. The net magnetic moment of the MPc molecules remains unchanged in MPc stripe/SiB. We find  $m = 0$  for NiPc stripe/ and ZnPc stripe/SiB and  $m = 1\mu_B$  for CuPc stripe/SiB. In NiPc stripe/SiB [Fig. 5(a)], we find electronic contributions of the Ni  $3d$  orbitals near the valence-band maximum, as well as at the conduction-band minimum, the latter being resonant with the Ni  $2p$  orbitals. However, the Zn  $3d$  orbitals present a lower contribution to the electronic states near the Fermi level [Fig. 5(c)]. The Zn  $3d$  orbital exhibits a DOS peak at  $E_F - 1.8$  eV, resonant with the (highest occupied) N  $2p$  orbital. As shown in Fig. 5(b), the net magnetic moment of CuPc stripe/SiB is due to the exchange splitting of  $\sim 0.8$  eV of Cu  $3d$  (mostly due to  $3d_{xy}$  and  $3d_{x^2-y^2}$ ) and N  $2p$  orbitals, giving rise to a net magnetic moment of  $1\mu_B$ . To establish if the magnetic state of the CuPc stripe/SiB is affected by the interactions between adjacent CuPc molecules, we performed the calculations with a  $2 \times 2$  square supercell containing four molecules and assigned the initial magnetization of each Cu atom, creating one ferromagnetic (all spins up) and three antiferromagnetic configurations (by combining two spins up and two spins down in all possible ways). Considering that the magnetic state remained unchanged when the self-consistent calculation finished and the final energies of all configurations were the same, we concluded that there is no magnetic coupling between molecules in the CuPc stripe/SiB. Based on the Bader analysis [50], we verified that at the CuPc stripe/SiB interface the net charge transfer is negligible ( $< 0.03e/\text{CuPc molecule}$ ).

To provide a quantitative picture of the contribution of the molecule-molecule and molecule-surface interactions to the formation of self-assembled stripes of CuPc on SiB, we calculate (i) the binding energy of a free-standing ML of CuPc stripes, keeping the equilibrium geometry of the CuPc stripe/SiB system, and (ii) the adsorption energy of a single CuPc molecule onto SiB, also keeping the equilibrium geometry of the CuPc stripe/SiB system while quadruplicating only the area of the SiB slab. In point (i), we took into account only the molecule-molecule interaction; that is, the CuPc-surface interaction has been turned off. However, in point (ii) the molecule-molecule interaction has been turned off, and we are computing just the (single) molecule interaction with the SiB surface. We find  $E^b = 1.54$  eV/molecule in point (i) and  $E^a = 0.78$  eV/molecule in point (ii); the sum of points (i) and (ii), 2.32 eV/molecule, is practically equal to the adsorption energy of the CuPc stripe/SiB system, 2.33 eV/molecule. We can infer that in the absence of chemical bonding, the formation energy of the self-assembled structure can be estimated by adding separately the two terms related to molecule-molecule and molecule-surface interactions [51–53]. By comparing points (i) and (ii), we find that the energetic stability of CuPc stripe/SiB is mainly due to the molecule-molecule interaction.

In Ref. [27], the authors found that CuPc molecules form a planar square (self-assembled) lattice, with a lattice constant of 14.5 Å, on Ag(100). Using the same considerations as the previous paragraph, to test the possibility of planar square CuPc array formation also on SiB, we examine the CuPc-CuPc interaction (the strength of CuPc-SiB interactions can be seen in Table II). We consider isolated free-standing molecules as depicted in Figs. 6(a)–6(d). Figures 6(a)–6(c) show three CuPc dimer configurations. In Fig. 6(d), we present a plausible periodic two-dimensional array of CuPc molecules in a square periodic lattice. Here it is worth noting that other periodic structures may form. For each geometry, the CuPc-CuPc equilibrium distance  $d$  and the atomic positions of the molecules were fully relaxed. For the CuPc dimer configurations, Figs. 6(a)–6(c), we find binding energies of 0.062, 0.040, and 0.012 eV/molecule, respectively. At  $T = 300$  K (room temperature), this also implies that the first two dimers are stable, presenting binding energies larger than the available thermal energy (0.026 eV). Meanwhile, for the square-lattice array [Fig. 6(d)], we find a binding energy of 0.428 eV/molecule, for an equilibrium distance  $d$  of 14.13 Å, namely, close to the one measured for the self-assembled square lattice of CuPc on Ag(100) [27].

There is no CuPc-CuPc chemical bonding among the CuPc molecules comprising the square-lattice array [Fig. 6(d)] or between the CuPc molecules and the SiB surface. For the array, we can estimate the binding energy by adding (i) the molecule-molecule interaction (neglecting the molecule-surface interaction) and (ii) the molecule-surface interaction (neglecting the molecule-molecule interaction), as we have done for the self-assembled CuPc stripe/SiB system. Here, for the (square) array system, we found 0.428 and 1.896 eV/molecule for points (i) and (ii), respectively. Consequently, the total binding energy per molecule is estimated to be 2.324 eV. The formation of planar square lattices and linear stripes on SiB is therefore energetically similar, suggesting that both structures may be found on SiB. The same scenario is expected for the other

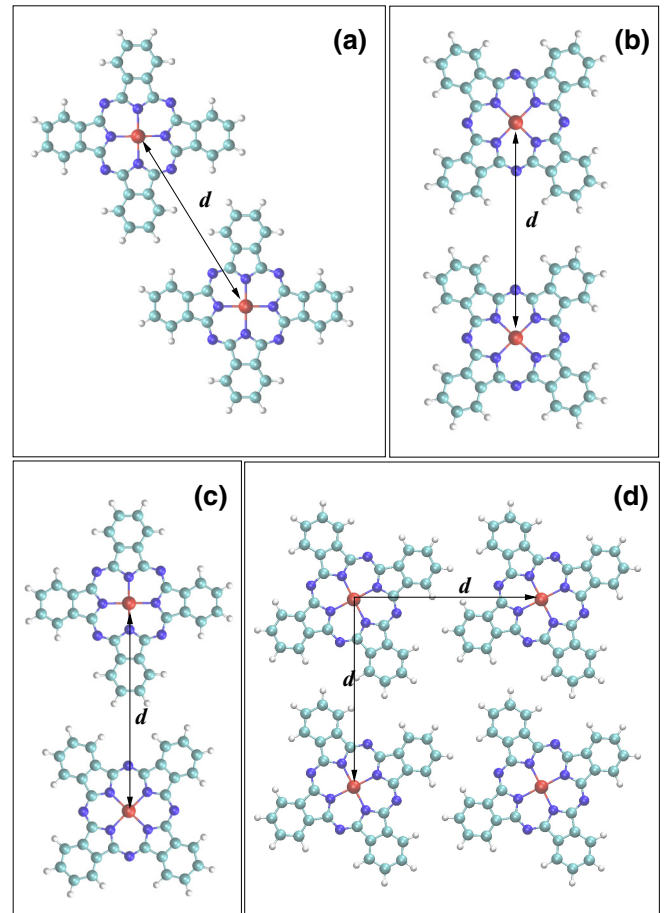


FIG. 6. (a)–(c) Structural models of (free-standing) CuPc dimers and (d) a periodic array of CuPc molecules; the equilibrium distances  $d$  are 14.54, 15.54, 15.10, and 14.13 Å, respectively.

molecules, NiPc and ZnPc on SiB. However, it is worth noting that we are examining only the energetic stability of the MPC molecules on SiB. Other aspects such as the activation energy barriers for diffusion, the growth temperature, and other surface boundary conditions might play an important role in the final equilibrium distribution and geometry of the molecules onto the surface. For instance, the presence of step edges on SiB promotes the formation of self-assembled stripes of ZnPc and CuPc molecules [24].

#### IV. SUMMARY

The results of *ab initio* calculations of metal-phthalocyanine molecules adsorbed on the Si(111)-B( $\sqrt{3} \times \sqrt{3}$ ) surface were presented. (i) We found that CrPc, MnPc, FePc, and CoPc form chemical bonds with the SiB surface provided that the metal atom is situated directly above the topmost Si adatom. (ii) In contrast, NiPc, CuPc, and ZnPc molecules are bound to the surface by only the vdW interaction. In point (i), upon the formation of MPC-SiB chemical bonds, the magnetic moment is quenched by  $1\mu_B$ . On the other hand, the magnetic moment remains unchanged in point (ii). The nature of the chemical interactions between the molecules and the surface was further examined by mapping the electronic charge transfers at the MPC-SiB interface, taking

CoPc/SiB ( $m = 1\mu_B \rightarrow 0\mu_B$ ) and CuPc/SiB ( $m = 1\mu_B \rightarrow 1\mu_B$ ) as illustrative cases. As a consequence of the weak vdW bonding, NiPc, CuPc, and ZnPc are expected to be able to quickly diffuse above the surface and they would therefore be expected to form supramolecular arrays, as has been reported in recent experimental studies of ZnPc and CuPc on Si(111)-B( $\sqrt{3} \times \sqrt{3}$ ) [24]. Based on these findings, we examined the energetic stability of self-assembled MPc stripes (M = Ni, Cu, and Zn) on the SiB surface. Those stripes are composed by MPc molecules separated by 4.1 Å parallel to the line direction, forming an angle of 38° (experiment  $\sim 30^\circ$ ) with respect to the surface. The energetic stability of those MPc stripe/SiB systems is mediated by (i) molecule-molecule and (ii) molecule-surface vdW interactions. In particular for CuPc stripe/SiB, we find that the contribution of interaction (i) is about two times greater than interaction (ii). A similar energy balance is expected for the other molecules, NiPc and ZnPc. Also, for the MPc stripe/SiB system, the magnetic moment of the molecules is not affected by the molecule-molecule interactions, thus revealing no magnetic coupling. Based upon interactions (i) and (ii), our total energy results suggest that we may also find SAMs composed by square lattices of CuPc, NiPc, and ZnPc molecules on the SiB surface, as observed for CuPc molecules on Ag(100) [27].

#### ACKNOWLEDGMENTS

The authors acknowledge financial support from the Brazilian agencies CNPq/INCT and FAPEMIG. R.G.A.V. gratefully acknowledges the FAPESP “Jovem Pesquisador em Centros Emergentes” Grant No. 2014/10294-4. The authors would like to acknowledge computing time provided on the Blue Gene/Q

supercomputer, supported by the Research Computing Support Group (Rice University) and Laboratório de Computação Científica Avançada (Universidade de São Paulo), as well as the computational facilities made available by CENAPAD/SP. The Natural Science and Engineering Research Council of Canada is also acknowledged for financial support.

#### APPENDIX

The presence of transition-metal atoms within the Pc skeleton suggests that correlation effects may be important. Therefore, the results of some of the previous calculations involving CoPc and CuPc were double-checked employing the DFT+ $U$  approach. The key parameter in these calculations is the effective Hubbard  $U$ , which we determined from first principles for the metal atoms using the linear response method that was proposed by Cococcioni and de Gironcoli [54], obtaining 5.88 and 7.82 eV for Co and Cu, respectively.

Overall, DFT+ $U$  yields the same spin states as uncorrected GGA calculations of CoPc and CuPc either in the gas phase or adsorbed on SiB, as previously depicted in Fig. 2(d). Of particular importance is the fact that the quenching of the CoPc magnetic moment (from  $1\mu_B$  to  $0\mu_B$ ) due to the formation of a Co-Si chemical bond was also reproduced by DFT+ $U$  calculations, as was the lack of magnetic coupling between adjacent molecules in the CuPc stripe/SiB system. Although the final occupation of  $d$  orbitals was slightly different because of the  $U$  term, the contribution of each orbital to the final magnetic states was unaltered. Therefore, these results suggest that the explicit consideration of electron correlations does not affect the conclusions presented in the main text of this work.

- 
- [1] S. M. Barlow and R. Raval, *Surf. Sci. Rep.* **50**, 201 (2003).  
 [2] S. D. Feyter and D. S. F. C., *Chem. Soc. Rev.* **32**, 139 (2003).  
 [3] J. V. Barth, G. Costantini, and K. Kern, *Nature (London)* **437**, 671 (2005).  
 [4] J. V. Barth, *Surf. Sci.* **603**, 1533 (2009).  
 [5] S. Fatayer, R. G. A. Veiga, M. J. Prieto, E. Perim, R. Landers, R. H. Miwa, and A. de Siervo, *Phys. Chem. Chem. Phys.* **17**, 18344 (2015).  
 [6] R. Wolkow, *Annu. Rev. Phys. Chem.* **50**, 413 (1999).  
 [7] I. R. McNab and J. Polanyi, *Chem. Rev.* **106**, 4321 (2006).  
 [8] J. R. Heath, *Annu. Rev. Mater. Res.* **39**, 1 (2009).  
 [9] A. Vilan, O. Yaffe, A. Biller, A. Salomon, A. Kahn, and D. Cahen, *Adv. Mater.* **22**, 140 (2010).  
 [10] B. Baris, J. Jeannoutot, V. Luzet, F. Palmino, A. Rochefort, and F. Chérioux, *ACS Nano* **6**, 6905 (2012).  
 [11] Y. Makoudi, F. Palmino, M. Arab, E. Duverger, and F. Chrioux, *J. Am. Chem. Soc.* **130**, 6670 (2008).  
 [12] O. Guillermet, A. Mahmood, J. Yang, J. Echeverria, J. Jeannoutot, S. Gauthier, C. Joachim, F. Chérioux, and F. Palmino, *ChemPhysChem* **15**, 271 (2014).  
 [13] S. R. Wagner and P. Zhang, *J. Phys. Chem. C* **118**, 2194 (2014).  
 [14] V. V. Korobtsov, V. G. Lifshits, and A. V. Zotov, *Surf. Sci.* **195**, 466 (1988).  
 [15] F. Thibaudau, P. Dumas, P. Mathiez, A. Humbert, D. Satti, and F. Salvan, *Surf. Sci.* **211–212**, 148 (1989).  
 [16] S. Bensalah, J. P. Lacharme, and C. A. Sébenne, *Surf. Sci.* **211–212**, 586 (1989).  
 [17] A. B. McLean, L. J. Terminello, and F. J. Himpsel, *Phys. Rev. B* **41**, 7694 (1990).  
 [18] F. Thibaudau, T. P. Roge, P. Mathiez, P. Dumas, and F. Salvan, *Europhys. Lett.* **25**, 353 (1994).  
 [19] P. Guaino, A. Cafolla, D. Carty, G. Sheerin, and G. Hughes, *Surf. Sci.* **540**, 107 (2003).  
 [20] P. Guaino, D. Carty, G. Hughes, P. Moriarty, and A. Cafolla, *Appl. Surf. Sci.* **212**, 537 (2003).  
 [21] J. A. Theobald, N. S. Oxtoby, M. A. Phillips, N. R. Champness, and P. H. Beton, *Nature (London)* **424**, 1029 (2003).  
 [22] S. Heutz, C. Mitra, W. Wu, A. J. Fisher, A. Kerridge, M. Stoneham, T. H. Harker, J. Gardener, H.-H. Tseng, T. S. Jones, C. Renner, and G. Aeppli, *Adv. Mater.* **19**, 3618 (2007).  
 [23] B. Amin, S. Nazir, and U. Schwingenschlögl, *Sci. Rep.* **3**, 1705 (2013).  
 [24] S. R. Wagner, R. R. Lunt, and P. Zhang, *Phys. Rev. Lett.* **110**, 086107 (2013).  
 [25] A. Zhao, Q. Li, L. Chen, H. Xiang, W. Wang, S. Pan, B. Wang, X. Xiao, J. Yang, J. G. Hou, and Q. Zhu, *Science* **309**, 1542 (2005).

- [26] L. Gao, W. Ji, Y. B. Hu, Z. H. Cheng, Z. T. Deng, Q. Liu, N. Jiang, X. Lin, W. Guo, S. X. Du, W. A. Hofer, X. C. Xie, and H.-J. Gao, *Phys. Rev. Lett.* **99**, 106402 (2007).
- [27] S. Stepanow, A. Mugarza, G. Ceballos, P. Moras, J. C. Cezar, C. Carbone, and P. Gambardella, *Phys. Rev. B* **82**, 014405 (2010).
- [28] J. Schaffert, M. C. Cottin, A. Sonntag, H. Karacuban, C. A. Bobisch, N. Lorente, J.-P. Gauyacq, and R. Moller, *Nat. Mater.* **12**, 223 (2013).
- [29] P. Giannozzi *et al.*, *J. Phys. Condens. Matter* **21**, 395502 (2009).
- [30] M. Dion, H. Rydberg, E. Schröder, D. C. Langreth, and B. I. Lundqvist, *Phys. Rev. Lett.* **92**, 246401 (2004).
- [31] T. Thonhauser, V. R. Cooper, S. Li, A. Puzder, P. Hyldgaard, and D. C. Langreth, *Phys. Rev. B* **76**, 125112 (2007).
- [32] G. Roman-Perez and J. M. Soler, *Phys. Rev. Lett.* **103**, 096102 (2009).
- [33] H. J. Monkhorst and J. D. Pack, *Phys. Rev. B* **13**, 5188 (1976).
- [34] P. Baumgärtel, J. J. Paggel, M. Hasselblatt, K. Horn, V. Fernandez, O. Schaff, J. H. Weaver, A. M. Bradshaw, D. P. Woodruff, E. Rotenberg, and J. Denlinger, *Phys. Rev. B* **59**, 13014 (1999).
- [35] H. Q. Shi, M. W. Radny, and P. V. Smith, *Phys. Rev. B* **66**, 085329 (2002).
- [36] D. P. Andrade, R. H. Miwa, B. Drevniok, P. Drage, and A. B. McLean, *J. Phys. Condens. Matter* **27**, 125001 (2015).
- [37] B. Białek, I. G. Kim, and J. I. Lee, *Thin Solid Films* **436**, 107 (2003).
- [38] B. Białek, I. G. Kim, and J. I. Lee, *Thin Solid Films* **513**, 110 (2006).
- [39] J. Wang, Y. Shi, J. Cao, and R. Wu, *Appl. Phys. Lett.* **94**, 122502 (2009).
- [40] X. Shen, L. Sun, Z. Yi, E. Benassi, R. Zhang, Z. Shen, S. Sanvito, and S. Hou, *Phys. Chem. Chem. Phys.* **12**, 10805 (2010).
- [41] O. I. Arillo-Flores, M. M. Fadlallah, C. Schuster, U. Eckern, and A. H. Romero, *Phys. Rev. B* **87**, 165115 (2013).
- [42] T. Kroll, R. Kraus, R. Schonfelder, V. Y. Aristov, O. V. Molodtsova, P. Hoffmann, and M. Knupfer, *J. Chem. Phys.* **137**, 054306 (2012).
- [43] P. Coppens, L. Li, and N. Zhu, *J. Am. Chem. Soc.* **105**, 6173 (1983).
- [44] N. Ishikawa, *Struct. Bonding* **135**, 211 (2010).
- [45] S. Stepanow, P. S. Miedema, A. Mugarza, G. Ceballos, P. Moras, J. C. Cezar, C. Carbone, F. M. F. de Groot, and P. Gambardella, *Phys. Rev. B* **83**, 220401 (2011).
- [46] M. Evangelisti, J. Bartolomé, L. J. de Jongh, and G. Filoti, *Phys. Rev. B* **66**, 144410 (2002).
- [47] The strain energy  $E^s$  is defined as  $E^s = E^{\text{strain}} - E^{\text{relax}}$ . The latter represents the total energy of the relaxed system, the free-standing MPC molecule, and  $E^{\text{strain}}$  represents the total energy of the strained MPC molecule. This term was calculated by keeping the atoms of the molecule at the same equilibrium geometry as that obtained for the McP/SiB adsorbed system.
- [48] We are aware that, in order to present a complete picture of the molecular diffusion on the surface, it is necessary to calculate the transition states of CuPc/SiB, which is beyond the scope of the present study.
- [49] In order to maintain the periodic boundary condition, within our supercell approach, we have considered a surface unit cell with orthogonal vectors ( $\beta = 90^\circ$ )  $\mathbf{a} = 6.70 \text{ \AA}$  and  $\mathbf{b} = 11.71 \text{ \AA}$ , where  $\mathbf{b}$  is rotated by  $30^\circ$  with respect to the  $[11\bar{2}]$  direction. In the experimental work [24], the authors measured lattice vectors of  $6.7$  and  $12.3 \text{ \AA}$  ( $\mathbf{a}$  and  $\mathbf{b}$ ), with  $\beta = 92^\circ$  and  $\mathbf{b}$  rotated by  $27^\circ$  with respect to the  $[11\bar{2}]$  direction.
- [50] R. Bader, *Atoms in Molecules: A Quantum Theory* (Oxford University Press, New York, 1990).
- [51] R. Otero, J. M. Gallego, A. L. V. de Parga, N. Martn, and R. Miranda, *Adv. Mater.* **23**, 5148 (2011).
- [52] M. Roos, B. Uhl, D. Künzel, H. E. Hoster, A. Groß, and R. J. Behm, *Beilstein J. Nanotechnol.* **2**, 365 (2011).
- [53] J. M. MacLeod and F. Rosei, *Small* **10**, 1038 (2013).
- [54] M. Cococcioni and S. de Gironcoli, *Phys. Rev. B* **71**, 035105 (2005).